Möller, P., Lüders, V., De Lucia, M. (2017): Formation of Rotliegend Ca-Cl brines in the North German Basin compared to analogues in the geological record. - *Chemical Geology*, *459*, pp. 32—42.

DOI: http://doi.org/10.1016/j.chemgeo.2017.04.001

Formation of Rotliegend Ca-Cl brines in the North German Basin compared to analogues in the geological record

P. Möller , V. Lüders, M. De Lucia

Helmholtz-Centre Potsdam, German Research Centre for Geosciences, Telegrafenberg, 14473 Potsdam, Germany

Corresponding author:

Peter Möller

Helmholtz-Centre Potsdam, German Research Centre for Geosciences, Section 3.4

Telegrafenberg

14473 Potsdam, Germany

Fone 0049/3312881430

Fax 0049/3312881529

Abstract: The formation of Ca-Cl brines is controlled by two major processes: chemical reactions between halite brines and igneous and metamorphic rocks and/or their debris in sedimentary basins, and the abstraction of H_2O by evaporation, freezing or formation of hydrous minerals. Albitization dominates in environments of low H_2O activity, i.e., halite saturated systems. Chloritization, serpentization and formation of smectites seems to be related to less saline systems, e.g., enhanced water activity.

The Rotliegend brines of the North German Basin evolved by interaction of infiltrating halite brines with volcanic debris of the Permian acid volcanic rocks by albitization of plagioclase. At present their temperatures are between 130 and 150°C at 3000-4000 m depth. Although they developed in a different environment they chemically and isotopically resemble the basinal brines from the Mississippi Salt Dom basin or even the deep brines from the Red Sea. All these brines have in common that halite brines interacted with plagioclase at enhanced temperatures. Their chemical composition is given by the reaction $An+SiO_2+2Na^+ \Leftrightarrow 2Alb+Ca^{2+}$. The trends of stable isotopes show slopes in the δD-$\delta^{18}O$ diagram which are typical for hydrothermal processes of evaporation brines with rock/sediments. The genesis of the Rotliegend brines differ from Ca-Cl brines in the Canadian Shield, Siberian Platform, the Dry Valleys in Antarctica and even the local brines from the Chilean salars and Bristol Dry Lake. The Siberian Platform and the Antarctic Dry Valley brines seem to be dominated by melting of ice-cements of their permafrost sections. The Ca-Cl brines of springs in the Chilean salars and the Bristol Dry Lake ascend due to thermal convection along tectonic faults. Although the Canadian Shield brines chemically resemble those of the Siberian Platform their stable isotope fractionation suggest that they developed by different processes of water abstraction. Some of the Canadian brines and the metamorphic KTB/VB brine may have gained their exotic stable isotope values by either small volume ratios of liquid and rocks, freezing or ultrafiltration processes.

Keywords: Ca-Cl brines; Generation of Rotliegend brines; North German Basin,

1. Introduction

The principle sources of seawater-derived Ca-Cl brines are dolomitization of limestones at enhanced temperatures (Iannace et al., 2012), chloritization and albitization of hot oceanic basalts (Schmidt et al., 2007; Tivey, 2007), serpentinization of ultrabasic material below 100°C of the mid oceanic ridges (Carlou et al., 2002; Batuev et al., 1994, Kelly et al., 2001) or interaction of mantle material and circulating seawater in the deep trench of the Red Sea (Pierret et al., 2001).

Evaporation of weathering solutions in closed basins initiates precipitation of carbonates, gypsum or sepiolite (Hardie and Eugster, 1970). During this process, three types of saline water develop that are either Na-Mg, Na-Ca or Na-HCO_3 dominated. These types of water reflect the heterogeneity of the local bedrocks undergoing weathering (Jones and Deocampo, 2003). Ephemeral inflows, springs and diffuse seeps feed playa lakes in intermontane basins. During evaporation mainly gypsum and halite build up mineral crusts. The remaining brines are mostly of Mg-Cl type such as in the salars of the Altiplano, Chile (Lowenstein and Risacher, 2009; Risacher et al., 2003; Boschetti et al., 2007), Salar de Uyuni, Bolivia (Sieland, 2014), the intermontane Qaidam Basin, northeastern section of the Plateau of Tibet (Spencer et al., 1990), the Lakes Amadeus, Tyrell and Eyre, Australia (Jacobson, 1988; Handford, 1982), the Great Salt Lake (Jones et al., 2009) and many other less spectacular ones.

Surface-near Ca-Cl brines seem to be restricted to tectonically active areas, where extreme diagenetic-hydrothermal Ca-Cl brines discharge such as, for example, in the Bristol Dry Lake and the Death Valley, USA (Handford, 1982; Lowenstein and Risacher, 2009), and in several springs of the salars of the Altiplano (Risacher et al., 2003), where volcanism and faulting provides the heat source and pathways for ascending brines. In the Dry Valleys of East Antarctica Ca-Cl brines are produced only few m below the surface by either cation exchange reactions along with freezing of soil solution (Matzubaya et al., 1979; Toner and Slettten, 2013) or by ascending low-temperature hydrothermal solutions that interacted with volcanic and/or crystalline rocks at depth (Lyons and Mayewski, 1993).

Different from sites, where Ca-Cl brines occur near surface, numerous drilling and mining activities proved the presence of Ca-Cl brines in the deep crust, e.g., Death Valley California, USA, (Lowenstein and Risacher 2009), Mississippi Salt Dome Basin (Kharaka et al., 1987; 2003), the Canadian Shield (Frape and Fritz, 1987; Bottomley et al 1999; Stotler et al., 2009),

the Siberian Platform (Alexeev et al., 2007) and the Bohemian Massif (Paces, 1987; Möller et al., 1997; 2005; Stober and Bucher 2005).

The Rotliegend brines in the North German Basin (NGB) are known from the Altmark gas field and the Groß- Schönebeck geothermal field (Fig. 1). The formation of these brines is still under debate (e.g., Gast, 1991; Gebhardt, 1994; Lüders et al., 2010; Regenspurg et al., 2016). The questions are how these Rotliegend brines evolved and are there modern analogues for comparison? Collecting information on actual playa brines and comparison of the chemical and stable isotope composition of Ca-Cl brines from different geologic settings may give insight into the development of Ca-Cl brines in general and of Rotliegend brines in the NGB in particular.

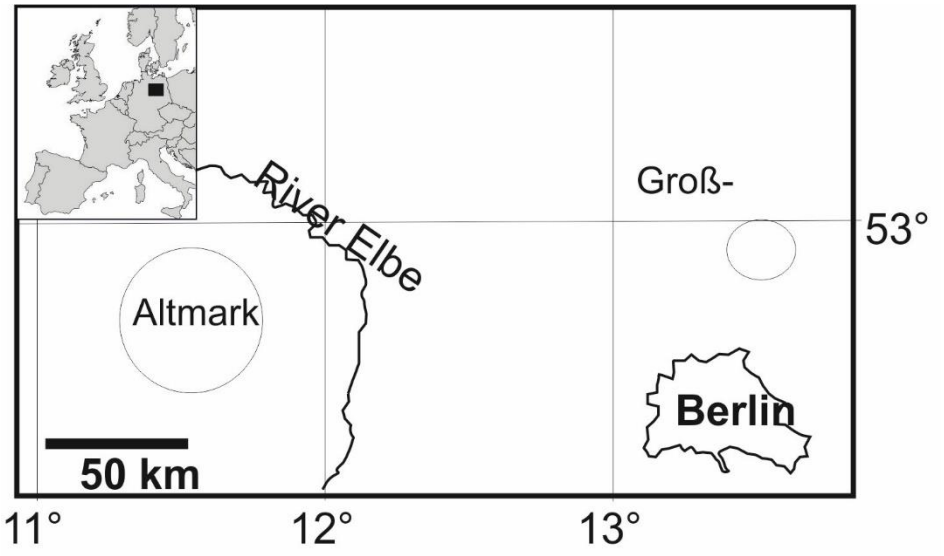

Fig. 1: Location of Altmark and Groß Schönebeck in North German basin.

2. Geological setting

The NGB covers the southern part of the Permian Basin (SPB) which is aligned broadly NW-SE, extending over a distance of 1700 km from onshore England, the southern North Sea, the Netherlands, and Northern Germany to the eastern border of Poland. It is situated between the Precambrian Baltic Shield in the north and the crystalline blocks of Cadomian, Caledonian, and Variscan age in the south. This basin is the largest depression worldwide (Warren 2008). The SPB evolved on rigid blocks of crystalline Cadomian and Variscan rocks and is filled with Paleozoic, Mesozoic, and Cenozoic sediments with up to 12 km thickness in its central part (Ziegler, 1977; Glennie, 1983; Ziegler, 1990). The SPB is characterized by differences in basement structure, sedimentary facies, and burial history. Beginning as a passive margin basin,

surrounded by stable cratons of Laurentia, Baltica and Gondwana, it evolved into an orogenic foreland basin due to the Variscan orgogeny in the Upper Carboniferous. Basin subsidence was interrupted only by stages of regional tectonic uplift and erosion in connection with Variscan folding, intense Lower Permian volcanism and major basin inversion phases at the Jurassic/Cretaceous boundary and during the Cretaceous.

Local late Upper Carboniferous–Early Permian extrusive acid magmatism was related to deeply penetrating crustal fracturing (Plein, 1978; Benek et al., 1996; Geißler et al., 2008). In general, the mineralogical composition of rhyolites and dacites is 18-35% quartz, 20-65% alkali feldspars, 3-40% plagioclase, up to 10% clinopyroxenes and rarely orthopyroxenes (Wimmenauer, 1985). The volcanic rocks of the Groß Schönebeck geothermal field plot in the field of dacites but show a trend line suggesting that magmatic differentiation of an original andesitic/trachy-andesitic melts developed into rhyolitic ones shown by increasing SiO_2, and decreasing Na_2O, CaO and Fe_2O_3 (Fig. 2). The erosion products of the volcanites accumulated in depressions between the volcanoes.

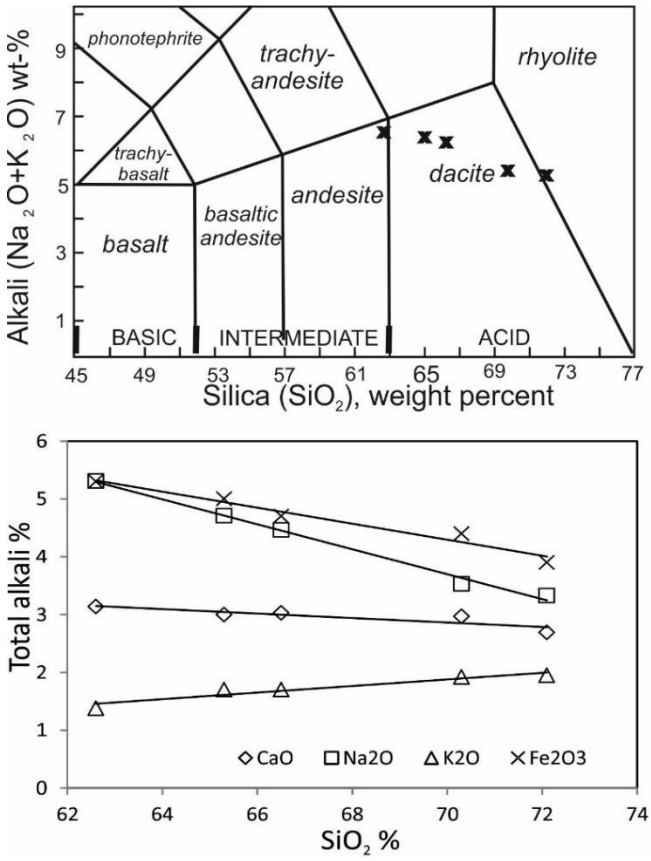

Fig. 2: Total-alkali–silica digram after Le Maitre et al (2002) (a). The variation of SiO_2, Na_2O, K_2O, CaO and Fe_2O_3 indicate the development of Mg-andesites to rhyolites (b).

At the beginning of the Permian, the climatic conditions changed from humid to arid and the sedimentation of in the SPB was dominated by continental siliciclastic red beds (Glennie, 1988). Poorly sorted conglomerates and eolian sediments are common. During the Upper Rotliegend a huge intracontinental playa lake covered areas of the southern North Sea through northern Germany (Gast, 1991). Lacustrine halite-rich evaporites which were very frequently drilled in wells in the southern part of the German North Sea and the North German Basin deposited under arid to semiarid conditions in this playa environment (Gast, 1991; Gebhardt 1994; Gaupp et al., 2000). The salty mud flats varied in area and chemical composition by either drying up or being enlarged during wet seasons (Gast, 1988; McCann, 1998). Abundant eolian depositions flank the southern margin of the SPB and are the most important reservoir units in the SPB gas province (Gaupp et al., 1993). The marine Zechstein transgression in the Upper Permian led to thick accumulations of carbonates, sulfates and salts representing the typical Zechstein evaporite cycles exceeding more than 2000 m thickness in the basin center. Subsequent subsidence of the basin is followed by new stages of rifting during the Triassic stage of extension (Brink et al., 1992; Brink, 2005; Van Wees et al., 2000). First diapirism of Zechstein salt was triggered by the great thickness of overlying Triassic sediments (Ziegler, 1977). During the Mid-Late Jurassic and Late Cretaceous–Early Tertiary, basin subsidence was interrupted by stages of major uplift (Ziegler, 1990). Late Cretaceous–Early Tertiary inversion mobilized Zechstein salt and led to the formation of numerous salt structures with local amplitudes of up to 8 km along NNE-SSW and NW-SE striking axis (Mohr et al., 2005). The local distribution of salt structures seems to play an important role in the evolution of basinal brines by water-rock interaction (Bennett and Hanor, 1987; Bein and Dutton, 1993; Kloppmann et al., 2001; Möller et al., 2008). After the inversion, major parts of the NGB underwent subsequent subsidence.

3. Features of Ca-Cl brines from various areas

The Ca-Cl brines dealt with in this contribution and their references are compiled in Table 1. Based on densities given in some references, the density as a function of total dissolved solids is derived. This function is used to calculate the missing densities in all the other analyses (App.1). All analyses, collected from references in Table 1 are converted into mmol/kgw. Applying PHREEQC and the Pitzer database (Parkhurst and Appelo, 2010) saturation indices of halite and gypsum and activities of Ca and Na are estimated.

Table1: Source of chemical and isotope composition of Ca-Cl brines from various locations

Location	I.D.	Depth of brines	Geology/lithology	Reference
North German Basin	NGB	Deep brines from boreholes		
-Altmark	NGB-Alt	3000-4000 m	Lower Rotliegend; acid volcanism; playa sediments	Lüders et al. (2010)
-Groß Schönebeck	NGB-GrSb			Regenspurg et al. (2016)
Canadian Shield	CS			
-Yellowknife	CS-Y			
-Thompson	CS-T	Brines from mines and boreholes	Crystalline basement and acid plutonism;	Frape & Fritz (1987)
-Sudbury	CS-S			
-Miramar	CS-M		Greenschist, amphibolites,	Bottomley et al. (1999)
-Lupin	CS-L		gneisses	Stotler et al. (2009)
Mississippi Salt Dome basin, USA	MSDB	Brines from boreholes, 2000-4400 m	Siliciclastic and carbonate sediments; evaporites	Kharaka et al. (1987)
Altiplano/Chile	Ch-Alt	Surface brines/salars	Active folding; acid volcanism	Risacher et al. (1999)
Red Sea/ Deep trench	RS	Deep brines, 2000-2500 m	Active Rift; Oceanic basalts	Pierret et al. (2001)
Bristol Dry Lake, USA	BDL	Diagenetic/hydrothermal brines from springs & boreholes		Handford (1982) Li et al (1997)
Death Valley, USA	DV			Lowenstein & Risacher (2009)
Dry Valleys, Antarctica	ANT			
-Lake Vanda	ANT-V	Surface brines	Soil & lake sediments	Webster (1994)Toner & Slotten (2013)
-Pond Don Juan	ANT-DJ			Matsubaya et al. (1979)
KTB-VB, Bohemian Massif Germany	KTB	Deep brines from boreholes	Metagabbros amphibolites	Möller et al. (1997; 2005); Stober and Bucher, 2005
Siberian Platform, Republik of Sacha	SP			
-Olenek area	SP-O	Brines from boreholes	Terrigenous carbonates, kimberlites,	Alexeev et al. (2007)
-Udachnaya area	SP-U		Terrigenous carbonates	

Logatchev vent fluids, Mid-Atlantic Ridge	Log	Sea floor ≈3000 m	Mantle rocks; sediments	Schmidt et al. (2007)

3.1 Spider diagrams

The spider diagrams reveal the dominance of Cl- in Ca-Cl brines (Fig.3). Mg is always less than Ca^{2+}. The Ca^{2+} concentrations are less than or equal to Na^{+} in brines from NGB, Canadian Shield, Mississippi Salt Dome basin, the Red Sea and the young brines from the Bristol Dry Lake, the Chilean Altiplano and the Salt Well in the Death Valley. Ca^{2+} is significantly higher than Na^{+} in the lakes of the Dry Valleys, Antarctica, in brines from the Olenek area in wester Yakutia and the 4000 m fluid from the deep KTB/VB well in the western Bohemian Massif, Germany. Although they differ in concentrations by three orders of magnitude, KTB/VB and vent fluids have striking extremely low Mg^{2+} concentrations. Although being different in origin, the Olenek and Antarctica brines resemble each other.

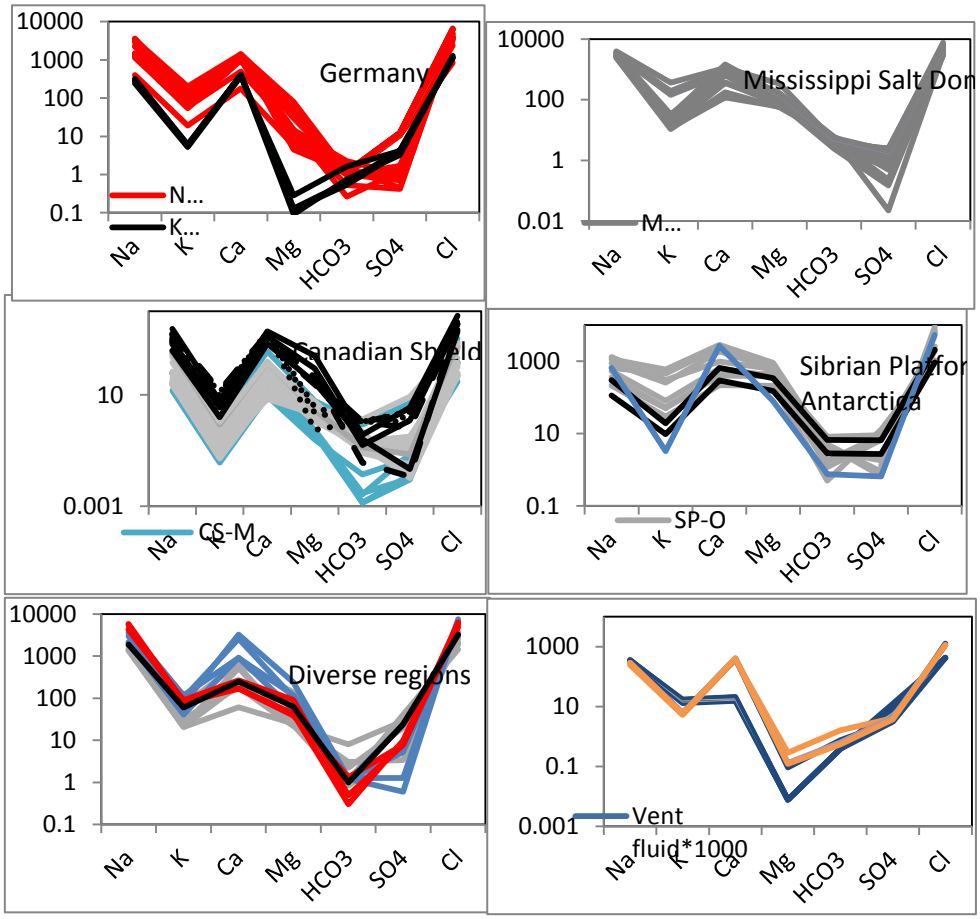

Fig. 3: Spider diagrams of Ca-Cl brines from North German Rotliegend (Lüders et al 2010), German part of the Bohemian Massif (Continental Deep Drilling Project) (Möller et al 1995) the Canadian Shield (Frape and Fritz 1987; Bottomley et al 1999; Stotler et al. 2009) Siberian Platform (Alexeev et

al 2007); Death Valley (Lowenstein and Risacher 2009), Antarctica (Toner and Sletten 2013; Red Sea (Pierret et al 2001) Salars , Chile (Risacher et al 1999).The vent fluids (Schmidt et al., 2007) are multiplied by a factor of 1000. Figures on Y axis are given in mmol/kgw. Identification of locations and corresponding references is given in Table 1.

3.2 [Na] vs [Cl] diagram

[Na] vs. [Cl] diagrams of Ca-Cl brines from different locations either scatter along individual correlation lines or cluster (Fig. 4a). Most of these brines are unsaturated with respect to halite. They represent either original unsaturated halite brines or are saturated halite brines that are diluted by saline/fresh water. Only the highest concentrations of Na^+ and Cl^- of the trend lines of RS, NGB, SP and CS achieve halite saturation as shown for seawater evaporation brines (McCaffrey et al., 1987).

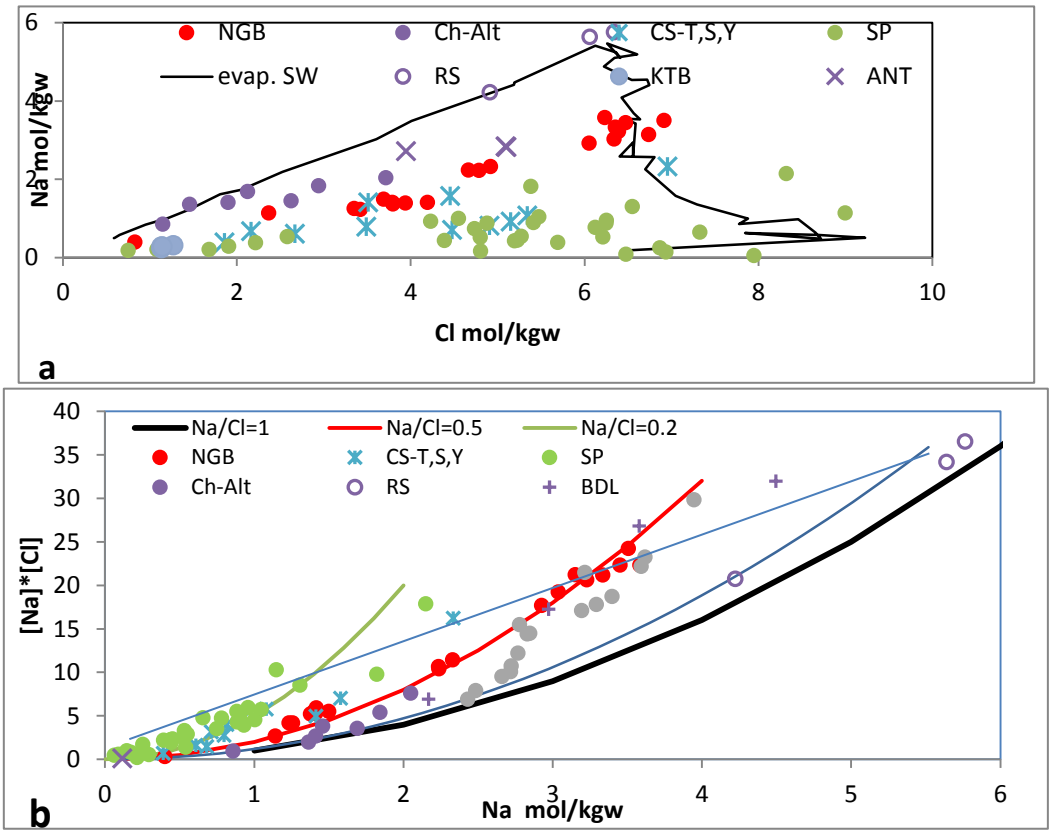

Fig. 4: Na-Cl correlation (a) The black line represents the evolution of Na^+ and Cl^- during seawater evaporation (evap. SW, McCaffrey et al. 1985). Identification of locations and corresponding references is given in Table 1. (b) Halite solubility. The blue line and curve are the results of seawater evaporation (McCaffrey et al. 1987); the bold, black line represents the estimated halite dissolution curve, Na/Cl=1.

The red and green curves represent evaporation of brines with Na/Cl of 0.5 and 0.2. Most samples plot between the respective evaporation curves and the linear halite saturation trend of seawater.

In a plot of [Na] vs. [Na]×[Cl], the evaporation trend of seawater below and beyond the saturation of halite is given as background information for discussing the composition of Na^+ and Cl^- concentrations of Ca-Cl brines (Fig. 4b). The Ca-Cl brines from the Red Sea represent a mixture of seawater-evaporation and the halite dissolution brines. The highest values indicate halite saturation of these mixtures. The NGB brines fit to the curve of Na/Cl at about 0.5; the MSDB brines fit to Na/Cl>0.5. The samples from the salars and Bristol Dry Lake approach the curve of NGB brines. At low Na concentrations the Ca-Cl brines of the Chilean salars fit the dissolution of stoichiometric halite but at enhanced molalities they develop into brines with Na/Cl of about 0.5. The brines from the Canadian Shield show final values of Na/Cl of about 0.3. Irrespective of the Na/Cl values of brines the highest products of Na^+ and Cl^- rarely plot beyond the solubility trend line of halite-saturated seawater. Most brines of the Bristol Dry Lake, Red Sea, the Canadian Shield, Siberian Platform and the Mississippi Salt Dome Basin are halite-saturated but only few from the NBG which is in agreement with Fig. 4a.

3.3 Correlation of Ca/Cl and Na/Cl

The trends of equivalent values of Na/Cl and Ca/Cl suggest that Ca^{2+} in solids is substituted by two Na^+ from solutions (Fig. 5). Assuming various starting ratios of variable Na and constant Cl of 1:1, 0.83:1, 1.1:1, and 0.5:1, increasing amounts of Na^+ exchanged for Ca^{2+}, □Na (Eq(1)) yield decreasing Na/Cl values and according Eq.(2) increasing Ca/Cl equivalent values. Most of the samples plot between the line of Na/Cl=1 and 0.83. The Na/Cl=0.5 fits the lowest ratios of the Siberian Platform. Only two samples from BDL and three from the Lupin mine, CS, plot beyond Na/Cl=1.1. All samples well above the Na/Cl=1 line indicate additional Ca^{2+}, e.g., dissolution of antarcticite (CaCl2.6H2O). Under atmospheric condition or when CO_2 is supplied from below, calcite precipitates and thus reduces the Ca^{2+} in brines. The Rotliegend brines are based on brines with Na/Cl between 12.0 and 0.8.

$$[Na]=[Na]_o-\Delta[Na] \quad (1)$$

$$[Ca]*2=[Ca]_o*2+\Delta[Na] \quad (2)$$

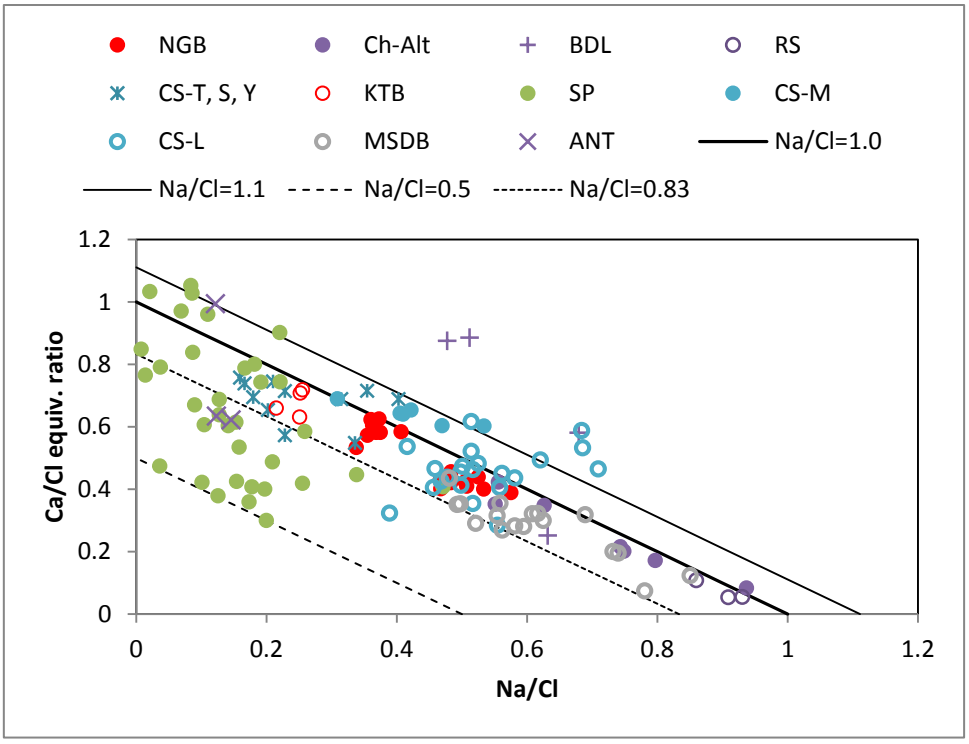

Fig. 5: Correlations of Na/Cl and Ca/Cl. The diffuse plot of equivalent ratios of Na/Cl vs Ca/Cl is structured by estimated exchange of Ca^{2+} against Na^{+} in brines with different Na/Cl values. For details see text. Identification of locations and corresponding references is given in Table 1.

3.4 Ca/Mg

Ca/Mg values are highly variable (Fig. 6). At Na/Cl<0.25 very high Ca/Mg values are given by brines from KTB and the Sudbury area, CS. At similarly low Na/Cl the samples from the Yakutian Olenek area, Siberian Platform, and Lake Vanda, Antarctica, plot below Mg/Ca of 3, both areas experience permafrost. In contrast, the Pond Don Juan brine, Antarctica, with temperatures as high as +26°C in deep water shows Ca/Mg values of 32. The deep brines from the Red Sea trench cluster at Ca/Mg values below 10 but at Na/Cl of about 0.9. Ca/Mg values of the other samples including NGB plot between 3 and 100 at intermediate Na/Cl values.

3.5 [Na]×[Cl] vs [Ca]×[Cl]^2

The correlation of the solute products [Na]×[Cl] and [Ca]×[Cl]^2 reveals different trends of brines from the NGB, CS, KTB/VB, MSDB and some springs of the Chilean salars. The samples from Miramar and Lupin, CS, represent brines either diluted by fresh water or being subjected to increasing evaporation before infiltration (Fig 7). The brines from the Siberian Platform and Bristol Dry Lake scatter but individual samples seem to depict the saturation of antarcticite. The NGB, Red Sea, and MSDB brines approach halite saturation. The solubility

products at saturation of halite and antarcticite are indicated by the limiting vertical and horizontal lines at values of about 30 and 230, respectively.

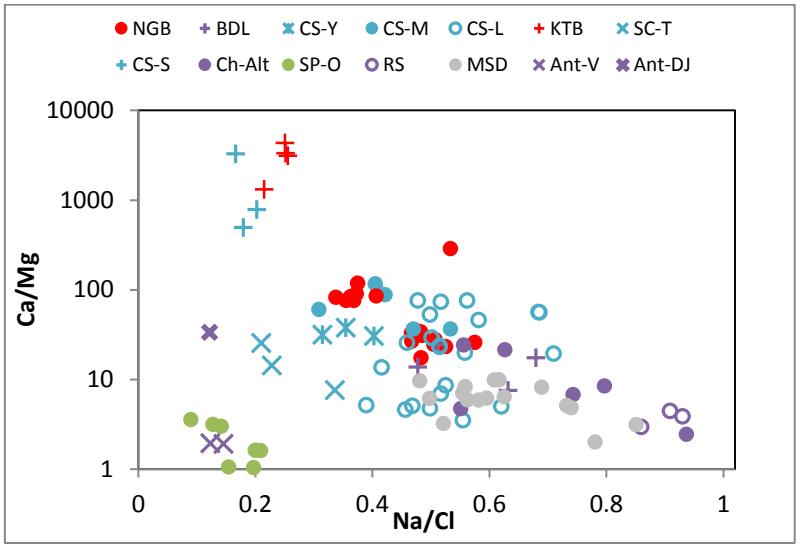

Fig. 6: Correlation of Na/Cl and Ca/Mg. Identification of locations and corresponding references is given in Table 1.

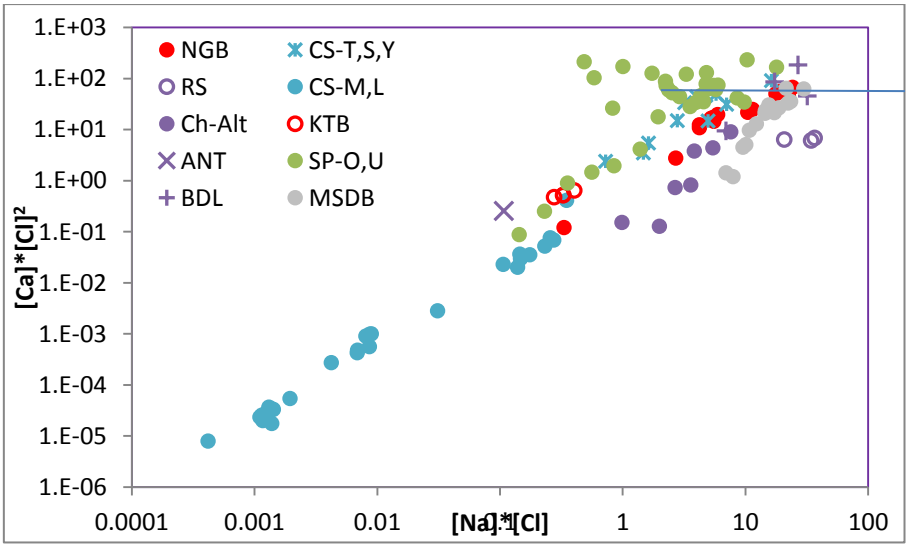

Fig. 7: Correlation of [Na]×[Cl] and [Ca]×[Cl]^2. The general upward trend culminates in the solubility products of halite, NaCl, and antarcticite, $CaCl_2{\cdot}6H_2O$ indicated by limiting lines. Note that brines from various locations do not follow the same trend line. Identification of locations and corresponding references is given in Table 1.

3.6 [Ca] vs [Ca]×[Cl]^2

Similar to Fig. 4b Ca is plotted vs [Ca]×[Cl]^2 (Fig. 8). Few data from Siberia and Antarctica plot along the dissolution curve of antarcticite. Bristol Dry Lake plots between Ca/Cl of 0.5 and

0.3. NGB brines fit to values of Ca/Cl about 0.25. Using the solubility product of antarcticite saturation of 230 from Fig. 7 and combining this point with the origin reveal that all data plot between two trends and, if not, near them (Fig. 8).

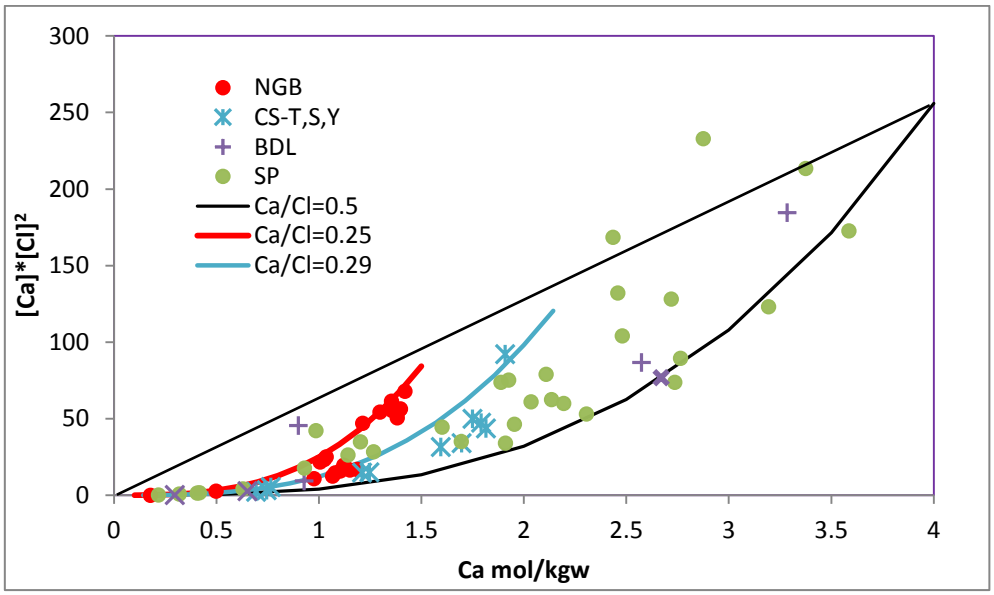

Fig. 8: The plot of Ca vs [Ca]×[Cl]^2 of Ca-Cl brines. Dissolution of antarcticite, Ca/Cl=0.5, is given by the black curve. Identification of locations and corresponding references is given in Table 1. mol/kgw

3.6 Br and Li relationship

Br and Li are the most conservative elements in evaporating systems. Values of Br/Cl and Li/Cl are high in deep brines hosted in metamorphites such as gneisses and metabasites that are intruded by granites, granodiorites, rhyolites or kimberlites (Fig. 9; for references refer to Table 1). Rotliegend brines from NGB gained Li by leaching lithium-rich mica, constituent of the Rotliegend volcanites. Low Li/Cl values are found in brines from mines in the Canadian Shield (CS-T, -S, -Y), i.e., rocks that lost soluble Li components during metamorphism. Low Br/Cl ratios are characteristic for brines from springs in salars and the Dry Valleys, Antarctica, i.e. leached sediments. 1000Br/Cl and 1000Li/Cl in most studied brines cluster between 0.1 and 10 and 1 and 10, respectively.

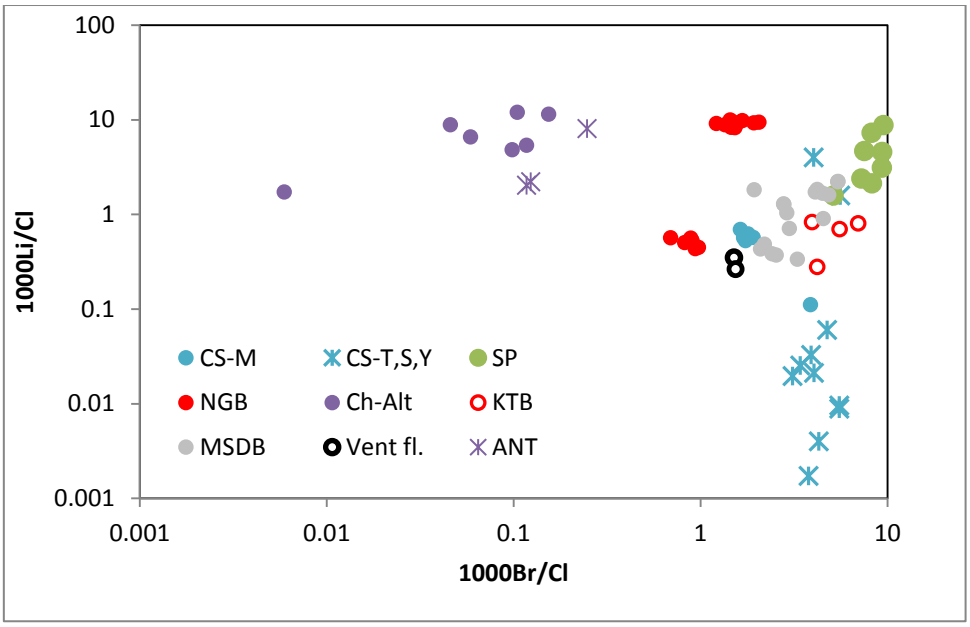

Fig. 9: Correlation of Li/Cl and Br/Cl. Identification of locations and corresponding references is given in Table 1.

Terrigenous evaporation brines generally show low Br/Cl values because halides are not abundant in igneous rocks and their debris in sediments (Fuge, 1978). Only interactions of brines with Br-rich organic sediments yield high Br/Cl values even exceeding those of highly evaporated seawater (Salameh et al., 2014). The highly variable Li^+ content may reflect the result of variable degrees of leaching of sediments, the precursors of the crystalline rocks. Precipitation of Li_2CO_3 by freezing of water reduces Li^+ in fluids; however, increasing temperatures enhances dissolution of Li_2CO_3. Only incorporation of Li^+ into alteration minerals may avoid increasing of Li^+ in the fluids. For example, eucryptite ($LiAlSiO_4$) is known to co-crystallize together with albite and and its formation may be a sink for Li^+ during albitization (Brush and Dana, 1880).

3.7 TDE-Na/Cl

When Na^+ is exchanged against Ca^{2+}, the salinity, given as TDS in g/l, decreases. Therefore, it is suggested to use the total dissolved equivalents, TDE, instead of TDS revealing dilution or mixing processes. In Fig. 10 TDE either clusters or plots along lines. The vertical downward trend indicates dilution by fresh water. Mixing with less saline waters might have occurred during sampling from bore holes, if not packer-defined sections are sampled or autoclaves were used. For instance, dilution by condensation of vapor is the reason for the wide vertical spread

of NGB brines from the Altmark wells. NGB brines from Groß Schönebeck, sampled during or after a long-time pumping tests, cluster. The Canadian Shield brines, collected in the mines Lupin and Miramar at temperatures below 0°C, suggest mixing with brines showing Na/Cl between 0.4 and 0.7. The brines being collected in the Thompson and Yellowknife mines at temperatures of about 20 °C (Fritz and Frape, 1982) show dilution by either fresh water or halite-bearing solutions. The samples from Lake Vanda and Pond Don Juan, Antarctica, represent dilution by melting ice-cements in soils. KTB fluid and Read Sea data cluster and thus indicate almost equilibrium with their host rocks. Decreasing TDE at increasing Na/Cl suggests dilution with brines with Na/Cl>1 such as in the Chilean salars and MSDB samples. MSDB brines scatter and seem to be altered by mixing with brines of variable halite contents. Brines from the Siberian Platform mixed with brines of Na/Cl of 0.2 or lost water by freezing due to which halite precipitated and Na/Cl decreased. Bristol Dry Lake is altered by mixing with Na/Cl about 1. The salars of the Chilean Altiplano and the Californian Bristol Dry Lake indicate by their trends that the substitution of Ca^{2+} against Na^{+} is enhanced by the evaporation of water.

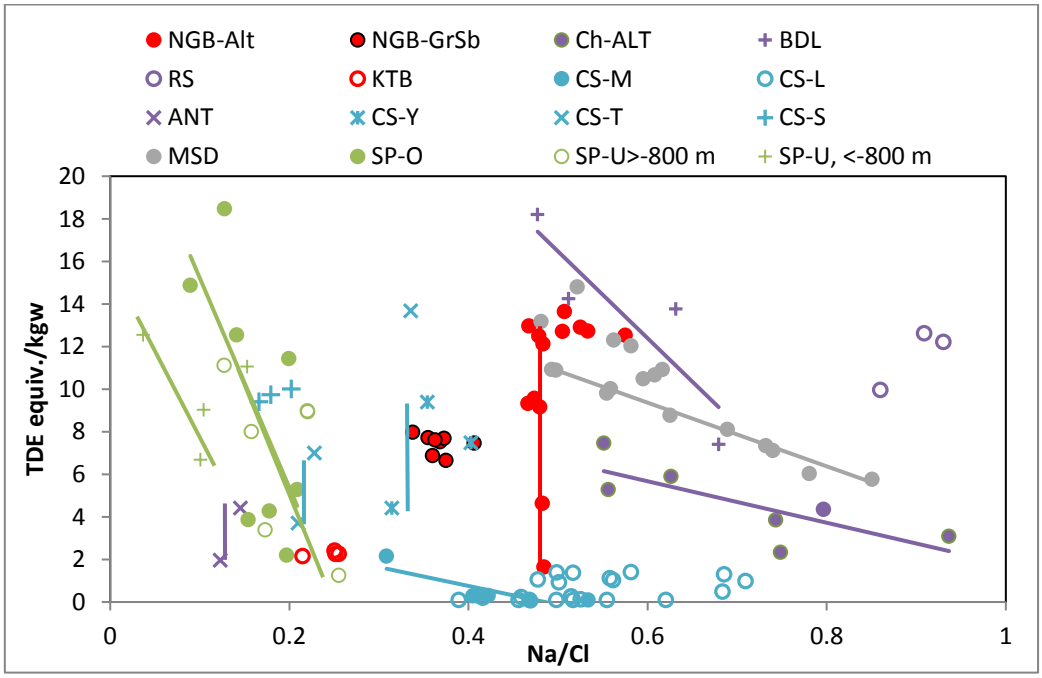

Fig. 10: Cross plots of TDE and Na/Cl. Dilution by fresh water is indicated by vertical downward trends, concentration by evaporation or freezing by inclined upward trends. Mixing with less saline waters might have occurred during sampling from bore holes, if not packer-defined sections are sampled. TDE decreasing with increasing Na/Cl indicate mixing with strongly saline waters. Identification of locations and corresponding references is given in Table 1.

3.7 δD and $\delta^{18}O$ fractionation

The δD and $\delta^{18}O$ values of brines either plot left or right to the global meteoric water line (GMWL), i.e., their slope is either greater or smaller than that of GMWL (Fig. 11). Irrespective of the initial δD and $\delta^{18}O$ isotope composition linear trends evolve by evaporation such as lines 1, 2, 3, 4 and 5 in Fig. 11a. Only evaporation brines that are very rich in Mg^{2+} and Ca^{2+} yield reversed trends (Sofer and Gat, 1972; 1975; Holser, 1979). For comparison the trends of δD vs $\delta^{18}O$ in water bodies connected to oceans such as the Baltic and Black Sea experience evaporation with slopes of about 7.2 (Fig. 11a). Endorheic systems like the Aral Sea, the Okavango Delta and even Lake Nasser, all located in the subtropical climate zone, show slopes between 5.4 and 5.9. These slopes resemble those of the brines from the Siberian Platform suggesting evaporation of continental run-off in probably pre-Pleistocene era.
NGB and MSDB basinal brines show a slope of about 2.4 and 2.0, respectively (Table 2). As known from hydrothermal alteration of sediments and rocks by infiltrating surface water yields slopes of about 2 (Giggenbach, 1992). The interstitial brines from Miocene/Pleistocene Red Sea sediments (Pierret et al., 2001) plot below GMWL with a slope of 0.8.

Slopes of about 3.6 are given by brines from the Dry Valleys, Antarctica, their ice-cement in soils and even one sample from the Siberian Platform. Based on the ice-cement the expected residual brine is estimated to plot left to the GMWL (Fig. 11b). It seems that the brines mainly represent molten ice-cement dissolving halite and antarcticite. The slopes of >8 are shown by brines from the Canadian Shield (except Miramar), few of the Siberian Platform and the KTB/VB. According to Kloppmann et al. (2002) "exotic stable isotope may be the rule in a restricted depth zone in all crystalline basements with slow groundwater movement but not too high temperatures".
There are three ways to explain these "exotic" stable isotope compositions plotting left to the GMWL:

- Very low water/rock ratios during crystallization of chlorite (Fritz and Frape, 1982) from high-salinity fluids (Graham and Sheppard, 1980; Gat, 1975) and possible formation of methane and H_2 by reaction with graphite (Bottinga, 1969; Richet et al., 1977).
- The combination of seawater evaporation and freezing is discussed by Bottomley et al (1999) and Kloppmann et al. (2002). The idea behind is that permafrost concentrates

dissolved species in the underlying brine by formation of ice and gas hydrates. Relic seawater might have been present in the sediments.

- Oxygen and hydrogen isotope fractionation of pressurized water passing compacted clay-rich sediments yield exotic δD and $\delta^{18}O$ values plotting beyond the GMWL (Coplen and Hanshaw. 1973)

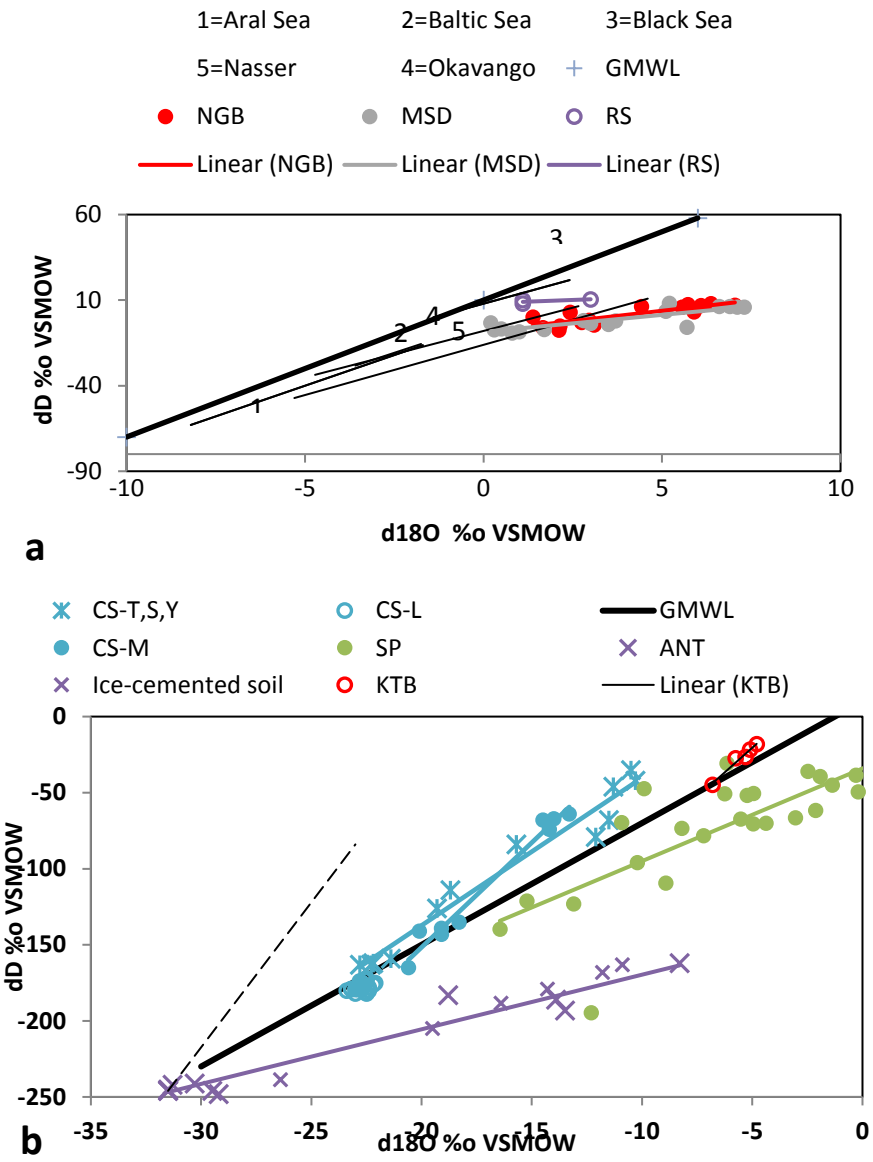

Fig. 11: Fractionation of δD and $\delta^{18}O$. Data for Ca-Cl brines are taken from references in Table 1. (a) For comparison the trends of actual evaporation systems are shown: 1=Baltic Sea (Bigg and Rohling, 2000; Schmidt 1999); 2=Black Sea (Rank et al., 1999); 3=Lake Nasser (Aly et al., 1993); 4=Okavango (Dincer et al., 1978); 5=Aral Sea (Oberhänsli et al., 2009). GMWL= global meteoric water line. (b) Data for the Canadian Shield, Siberian Platform, Antarctica and KTB/VB. For identification of locations refer to Table 1.

Table 2: Compilation of important parameters and resulting types of alteration reaction(s).

Location identification	Temperature at sampling site or downhole	Depth of sampling m	Slope od regression line in (Fig. 11), and processes involved	Saturation achieved for (Fig. 7)	Exponent *b* of $^{a}Na^{b}$ in $^{a}Ca/^{a}Na^{b}$ in Fig. 12	Probable type of dominant reactions
NGB	130-150	3000-4300	2.4; evaporation; hydrothermal W/R	halite	1.56	albitization, chloritization[a]
CS-T,-S,-Y	?		9.7	halite	1.7	albitization
Ch-Alt	>10	surface	evaporation		2.6	albitization
MSDB	75-121	1900-4300	2; evaporation; hydrothermal W/R	halite	2.6	albitization, Ca-Na ion exchange[b]
BDL	>20	surface		halite, antarcticite	2.3	albitization
SP	-1 to -8	200-2300	6.1; evaporation	antarcticite	2.26	albitization
RS	>20	2300	0.8; evaporation; hydrothermal W/R	halite	0.91	albitization, serpentization
CS-L	?	900-1100	Cluster Low fluid/rock ratio		0.72	amphibolite facies metamorphism[c]
CS-M	?	1400-1600	14		1.06	kaolinitization, chloritizaion
ANT	3-21	surface	3.6		1.15	
Log	70-300	surface Sea floor; ≈3000 m	melting ice-cement; cluster			chloritization, serpentinization[d]
KTB/VB	119	4000	cluster	Epidote, prehnite	0.4	amphibolite facies metamorphism[e]

[a] Fischer at al.,2012; [b]Kharaka et al., 2003; [c]Stotler et al., 2009; [d]Schmidt et al., 2007; [e]Möller et al., 2005; Stober and Bucher 2005.

Slopes of about 3.6 are given by brines from the Dry Valleys, Antarctica, their ice-cement in soils and even one sample from the Siberian Platform. Based on the ice-cement the expected residual brine is estimated to plot left to the GMWL (Fig. 11b). It seems that the brines mainly represent molten ice-cement dissolving halite and antarcticite. The slopes of >8 are shown by brines from the Canadian Shield (except Miramar), few of the Siberian Platform and the KTB/VB. According to Kloppmann et al. (2002) "exotic stable isotope may be the rule in a restricted depth zone in all crystalline basements with slow groundwater movement but not too high temperatures".

There are three ways to explain these "exotic" stable isotope compositions plotting left to the GMWL:

- Very low water/rock ratios during crystallization of chlorite (Fritz and Frape, 1982) from high-salinity fluids (Graham and Sheppard, 1980; Gat, 1975) and possible formation of methane and H_2 by reaction with graphite (Bottinga, 1969; Richet et al., 1977).
- The combination of seawater evaporation and freezing is discussed by Bottomley et al (1999) and Kloppmann et al. (2002). The idea behind is that permafrost concentrates dissolved species in the underlying brine by formation of ice and gas hydrates. Relic seawater might have been present in the sediments.
- Oxygen and hydrogen isotope fractionation of pressurized water passing compacted clay-rich sediments yield exotic δD and $\delta^{18}O$ values plotting beyond the GMWL (Coplen and Hanshaw. 1973)

4 Discussion

Among the igneous minerals plagioclase is unstable at low temperatures in the presence of water and CO_2 and is converted to minerals that are more stable under ambient conditions. There are many reactions such as (3)–(8) but albitization of plagioclase is considered to be the most prominent one in the presence of halite brines. Having this in mind, the activities of Ca^{2+} and Na^+ are correlated in Fig. 12 and the trend lines of brines from each location are displayed. These trend lines in the anti-logarithmic plot correspond to exponential functions.

Two groups of slopes evolve which have either final exponent *b* of $^aNa^+$ of about 2 or below 1.2 (Table 3). The corresponding pre-exponential factors *a* range from 2.7 to 0.1. The alteration reactions (3)–(8) are discussed:

$$\underset{\text{Anorthite}}{CaAl_2Si_2O_8} + 2Na^+ + 4SiO_2 \Leftrightarrow \underset{\text{Albite}}{2NaAlSiO_8} + Ca^{2+} \quad (3)$$

$$CaAl_2Si_2O_8 + 2H^+ + H_2O \Leftrightarrow \underset{\text{Kaolinite}}{0.5Al_4Si_4O_{10}(OH)_8} + Ca^{2+} \quad (4)$$

$$CaAl_2Si_2O_8 + 5Mg^{2+} + SiO_2 + 8H_2O \Leftrightarrow \underset{\text{chlorite}}{Mg_5Al_2Si_3O_{10}(OH)_8} + Ca^{2+} + 8H^+ \quad (5)$$

$$\underset{\text{diopside}}{CaMg[Si_2O_6]} + 3Mg^{2+} + 4\,H_2O \Leftrightarrow \underset{\text{serpentine}}{Mg_3[(OH)_4Si_2O_6]} + Ca^{2+} + 4H^+ \quad (6)$$

$$2CaAl_2Si_2O_8 + 2Na^+ + 2H^+ + 4SiO_2 + H_2O \Leftrightarrow 2NaAlSiO_8 + 0.5Al_4Si_4O_{10}(OH)_8 + 2Ca^{2+} \quad (7)$$

$$2CaAl_2Si_2O_8 + 2Na^+ + 5Mg^{2+} + 5SiO_2 + 8H_2O \Leftrightarrow Mg_5Al_2Si_3O_{10}(OH)_8 + 2NaAlSi_3O_8 + 2Ca^{2+} + 8H^+ \quad (8)$$

The equilibrium constant K of reaction (3) is given by Eq.(9) for quartz as the reactant. Reactions (4), (5) and (6) yield Ca^{2+} without changes in Na^+. Reactions (5) and (6) consume Mg^{2+}. In the reactions of concurrent albitization and kaolinitization (7) or chloritization (8) K is proportional to $^aCa/^aNa$. Thus albitization of plagioclase and the concurrent reactions with additional formation of either kaolinite or chlorite seems to explain the two groups of slopes emerging in Fig. 12.

$$\log(K) = \mathrm{Log}(^aCa/^aNa^2) \quad (9)$$

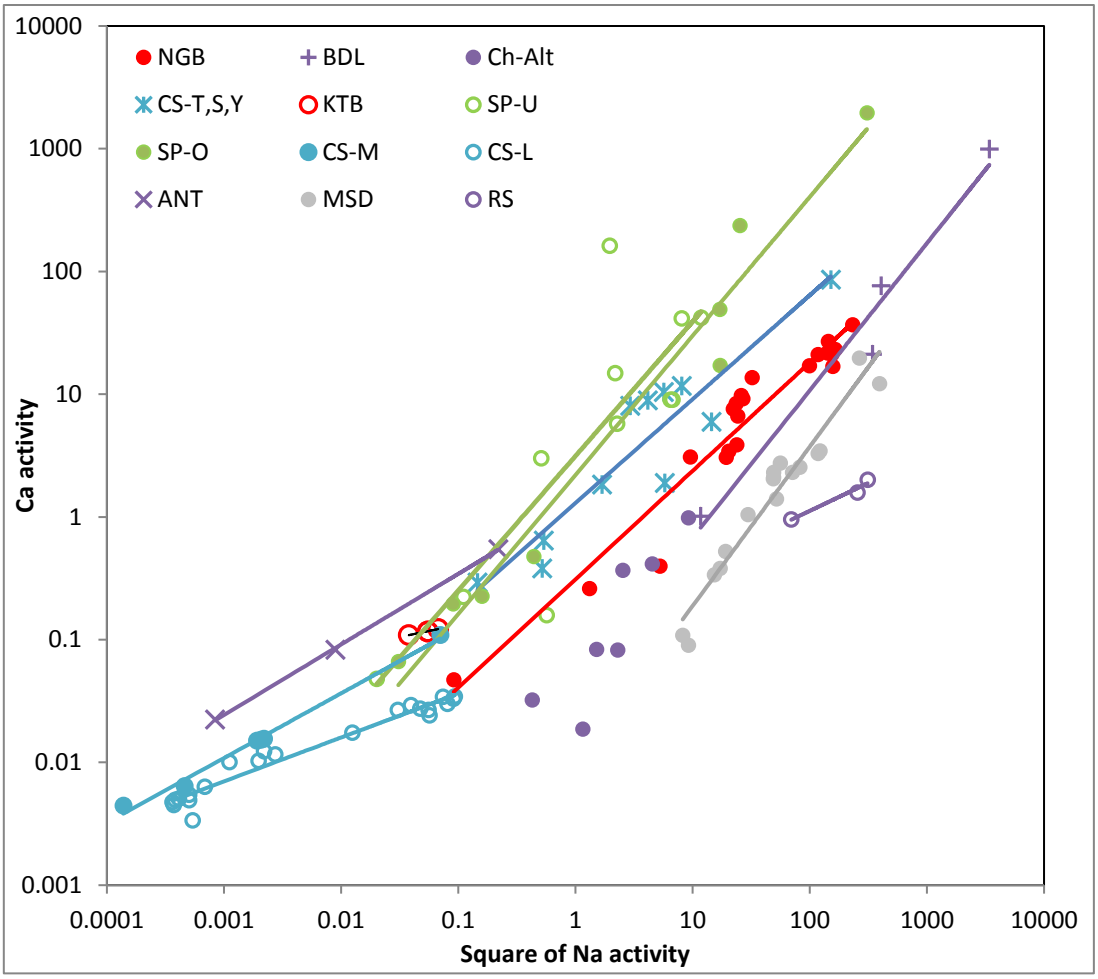

Fig. 12: Activity plot of Na vs Ca. Activities are estimated after PHREEQC using the Pitzer data base (Parkhurst and Appelo, 2010). Identification of locations and corresponding references is given in Table 1. For details see text.

If Ca^{2+} is partially precipitated, e.g., as calcite, K is no longer proportional to ${}^{a}Ca/{}^{a}Na^{2}$ but to ${}^{a}Ca^{(1-x)}/{}^{a}Na^{2}$ or ${}^{a}Ca/{}^{a}Na^{2/(1-x)}$. Thus, with x<1 the exponent of ${}^{a}Na$ increases and vice versa. If Ca^{2+} is gained by additional reactions, the exponent of ${}^{a}Na$ decreases. This explains the variation from the exponent *b*=2 in Table 3.

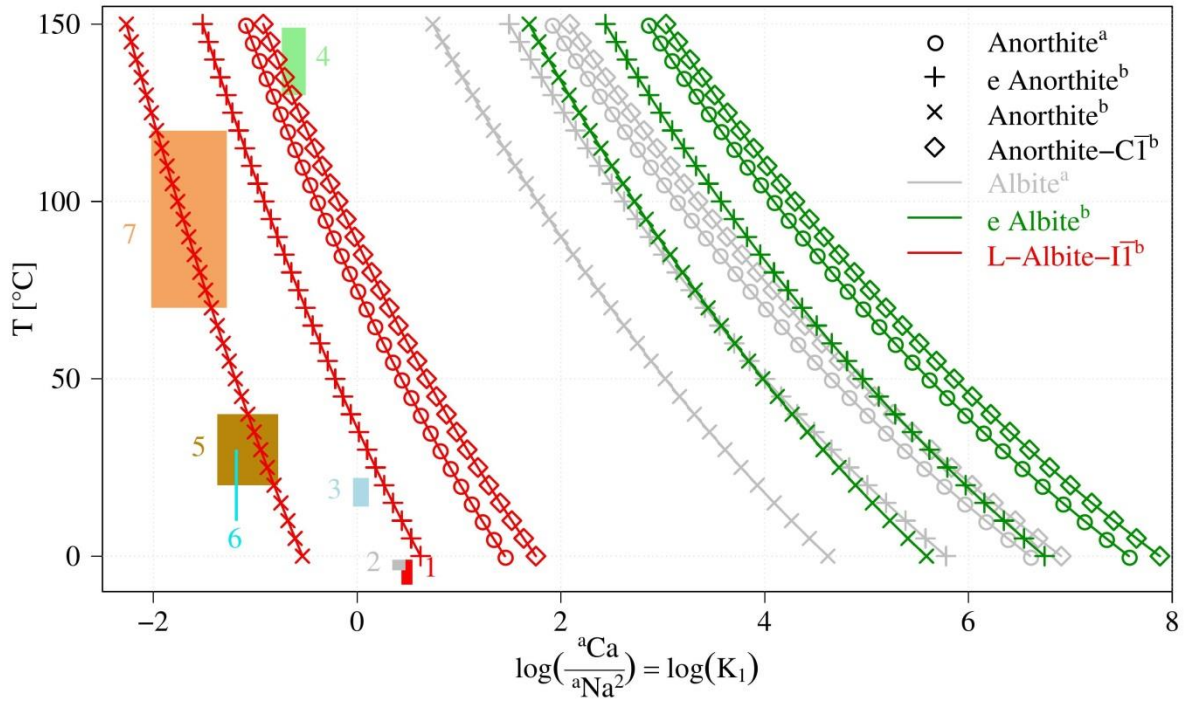

Fig. 13: Plot of estimated values of log($^{a}Ca/^{a}Na^{2}$) of brines involved in albitization reaction. Here different scenarios are given by combinations of various modifications of anorhite (indicated by symbols) and resulting albite (indicated by colored lines). [a]refers to thermodynamic data of Helgeson et al. (1978) and Shock et al. (1988); [b]refers to data from Arnorsson and Stefansson (1999); e= endmember; pure anorthite and albite. The vertical bars show the results of log($^{a}Ca/^{a}Na^{2}$)=log(a) (Table 3) vs. their corresponding present-day temperatures Table 2. Log(a) based on chemical analyses reasonably fit the estimated log(K) values based on the thermodynamic data of Arnorsson and Stefansson (1999). Deviations may be due to non-equilibrium particular at low temperatures and additional concurrent reactions (see text).

Table 3: Results of trend lines of the type $y=ax^b$ in Fig. 12. Two groups of exponents with either about 2 or about 1 emerge.

		Trend line $Y=aX^b$		
ID in Fig. 13	Location	Exponent *b*	Pre-factor *a*	Regression coef. R^2
1	NGB-Alt	1.54	0.091	0.97
2	NGB-GrSb	1.57	0.12	0.91
3	MSDB	2.6	0.0096	0.94
4	Ch-Alt	2.6	0.049	0.78
5	BDL	2.34	0.043	0.96
6	CS-T, S, Y	1.7	1.22	0.87
7	SP-O	2.26	2.22	0.97
	ANT-V	1.15	1.3	0.99
	CS-M	1.06	0.42	0.99
	CS-L	0.72	0.084	0.96
	RS	0.91	0.14	0.96
	KTB	0.3	0.1	0.99

The values of log(K) in Eq. (9) is estimated by applying the CHNOSZ program (Dick, 2008) using either the thermodynamic data from Helgeson et al. (1978) and Shock et al. (1988) or as defaults those of albite and anorthite modifications from Arnorsson and Stefansson (1999). The original database yields significant higher values of log(K) than when using the implemented ones (Fig. 13). The maximal temperature of the brines discussed in this contribution is about 150°C. Under these conditions high-albite does not form. High-temperature anorthite modifications are only reasonable in basalts but not in plutonic or metamorphic rocks due to their slow cooling rates during which the high formations are converted to the low-temperature ones. The combinations of the various thermodynamic data of anorthite and albite yield a wide spread of log(K). The values of $^{a}Ca/^{a}Na$ and the corresponding temperature range taken from Fig. 12 and Table 2, respectively, only fit the thermodynamically derived log(K) based on data from Arnorsson and Stefansson (1999). When plotting the analytical results into Fig. 13 it is assumed that equilibria exist which may be true for the brines with enhanced temperatures but not for the low temperature ones.

In Table 2 the most important parameters of the discussed brines are compiled. There are two groups: those that dominantly are based on albitization of anorthite and those based on combined reactions of anorthite to albite and kaolinite or chlorite. The first group seems to

depend on precipitation evaporated to brines by reaction of plagioclase under surface conditions like in salars and BDL or after heated during descend like in NGB and MSDB. All these brines are halite and or antarcticite saturated (if not diluted thereafter) and thus their H2O activity is low.

In group 2 all brines are unsaturated with respect to halite and thus the activity of water is high. Therefore kaolinitization, chloritization and serpentinization occur concurrent with albitization. Precipitation directly infiltrated (CS-L) or water was abstracted by processes such as low water/rock interaction (KTB; Simon and Hoefs, 1993), ultrafiltration (Coplen and Hanshaw, 1973) or freezing (Antarctica, Siberian Platform).

Thus these two types of reactions cover the spread of exponents of ^{a}Na in Fig. 12. Uncertainties are probably due to minor concurrent reactions like (7) and (8) and analytical uncertainties in sampling either by dissolving calcites particles by acidification of unfiltered samples or by storage of non-acidified samples in which calcite might have precipitated.

5 Conclusion

During the Upper Rotliegend, playa lakes formed in central depressions of the Southern Permian Basin under arid to semiarid conditions. Similar to modern playas in the Chilean Altiplano ephemeral saline pools occupied variable areas of wide mudflats across the depressions. At the surface salt crusts formed from evaporating brines. Some meters below the playa surface, the confined aquifer was filled with interstitial brine, whose capillary draw precipitated a variety of salts within the sediment such as gypsum, halite and probably even antarcticite. The dissolved inorganic carbon was reduced by precipitation of calcite. Sulfate is reduced by precipitation of gypsum. CO_2 in open systems was controlled by the atmosphere, biologically produced or mantle-derived CO_2. By their gravity these halite brines infiltrated and interacted with sedimentary debris of Rotliegend volcanic rocks filling the depressions between the volcanoes or the volcanites themselves yielding finally Na/Cl of 0.4–0.5 by alteration of plagioclase to albite. The trend of δD and $\delta^{18}O$ and $^{a}Ca/^{a}Na^{2}$ suggest that albitization occurred at enhanced temperatures. At present-day temperatures of 130 -150°C equilibrium may be achieved. The trend of δD and $\delta^{18}O$ and chemical features in Figs. 3–7 and 12 resembles those of basinal brines from the Mississippi Salt Dome basin (Fig. 11).

Ca-Cl brines are formed essentially by either dominant albitization or albitization in concurrence with kaolinitization, chloritization and serpentinization depending on the H_2O activity of the system. The playa lakes of the environment of NGB are subjected

evaporation/dissolution cycle similar to those of the Bristol Dry Lake and Chilean salars but their brine compositions were different. In the Altiplano and in the Bristol Dry Lake the Ca-Cl brines are transported by thermal convection to the surface, where minerals such as antarcticite form by extreme evaporation of water. Dissolution of these mineral crust yield Ca enriched brines at the surface. Contrasting, the NGB halite brines infiltrated and reacted with plagioclase at enhanced temperatures in the sediment pile. The reacting brines are more or less halite-saturated, i.e., the H_2O activity is low.

Abstraction of water by mineral reactions under low brine and rock volume ratio played a role in generation of the KTB/VB 4000 m fluid (Simon and Hoefs, 1993). Most of the brines from the Canadian Shield and few ones of the Siberian Platform are either influenced by permafrost or ultrafiltration.

References

Alexeev S.V., Alexeeva, L.P., Borisov, V.N., Shouakar-Stash, O., Frape, S.K., Chabaux, F., Kononov, A.M., 2007. Isotopic composition (H, O, C, Sr) of ground brines of the Siberian Platform. Russ. Geol. Geophys. 48, 225–236.

Aly, A.I.M., Froehlich, K., Nada, A., Hamza, M., Salem, W. M., 1933. Study of environmental isotope distribution in the Aswan High Dam Lake (Egypt) for estimating the evaporation of lake water and its recharge to adjacent groundwater. Environ. Geochem. Health 15, 37–49.

Arnorsson, S., Stefansson, A., 1999. Assessment of feldspar solubility constants in water in the range 0° to 350°C at vapor saturation pressure. Amer. J. Sci. 299, 173–209.

Batuev, B.N., Krotov, A.G., Markov, V.F., Cherkashev, G.A., Krasnov, S.G., Lisitzin, Y.D., 1994. Massive sulfide deposits discovered at 14°45'N, Mid-Atlantic Ridge. BRIDGE Newslet. 6, 6–10.

Bein, A., Dutton, A.R., 1993. Origin, distribution, and movement of brine in the Permian Basin (U.S.A.): A model for displacement of connate brine: Geol. Soc. Amer. Bull. 105, pp. 695.

Benek, R, Kramer, W., McCann, T., Scheck, M, Negendank, J, Korich, D, Huebscher, H., Bayer, U, 1996. Permo-carboniferous magmatism of the Northeast German Basin. Tectonophysics 266, 379–404.

Bennett, S.S., Hanor, J.S., 1987. Dynamics of subsurface salt dissolution at the Welsh Dome, Lousiana Gulf Coast, in: Lerche, L., O'Bian, J.J. (Eds), Dynamical geology of salt and related structures. Academic Press, Orlando, pp 653–677.

Bigg, G. R., Rohling, E. J., 2000. An oxygen isotope data set for marine water. J. Geophys. Res. 105, 8527–8535.

Boschetti, T., Cortecci, M., Barbieri, M., Mussi, M., 2007. New and past geochemical data on fresh to brine waters of the Salar de Atacama and the Andean Altiplano, northern Chile. Geofluids 7, 33–50.

Bottinga, Y., 1969. Calculated fractionation factors between carbon and hydrogen isotope exchabge in the system calcite-carbon dioxide-graphite-methane-hydrogen-water-vapor. Geochim. Cosmochim. Acta 33, 49–64.

Bottomley, D.J., Katz, A., Chan, L.H., Starinsky, A., Couglas, M., Clark, I.D., Raven, K.G., 1999. The origin and evolution of Canadian Shield brines: evaporation or freezing of seawater? New lithium isotope and geochemical evidence from the Slave Lake craton. Chem. Geol. 155, 295–320.

Brink, H.J. (2005) The evolution of the North German Basin and the metamorphism of the lower crust. Int. J. Earth Sci. (Geol. Rundsch.) 94, 1103–1116.

Brink, H.J., Dürscher, H., Trappe, H., 1992. Some aspects of the late- and post-Variscan development of the North German Basin. Tectonophysics 2007, 65–95.

Brush, G.J., Dana, E.S., 1880. On the mineral locality at Branchville, Connectica: fourth paper Spodumene and the results of alteration. Am. J. Sci., third series, XX, 257–285.

Calou, J.L., Donval, J.P., Fouquet, Y., Jean-Baptiste, P., Holm, N., 2002. Geochemistry of high H_2 and CH_4 vent fluids issuing from ultramafic rocks at the Rainbow hydrothermal field (36°14'N, MAR). Chem. Geol. 191, 345–359.

Coplen, T.B., Hanshaw, B.B., 1973. Ultrafiltration by compacted clay menbran. I. Oxygen and hydrogen isotopic fractionation. Geochim. Cosmochim. Acta 37, 2295–2310.

Dick, J.M., 2008. Calculation of the relative metastabilities of proteins using the CHNOSZ software package. Geochemical Transactions 9:10; doi: 10.1186/1467-4866-9-10

Dinçer, T., Hutton, L.G., Kupee, B.B.J., 1978. Study, using stable isotopes, of flow distribution, surface-groundwater relations and evapotranspiration in the Okavango Swamp, Botswana. Proc. Int. Symp. International Atomic Energy Agency, Neuherberg, pp. 3-26.

Frape, S.K., Fritz, P., 1987. Geochemical trends for groundwaters from the Canadian Shield, in: Fritz, P., Frape S.K. (Eds), Saline water and gases in crystalline rocks. Geol. Ass. Canada Spec. Pap. 33, 19–38.

Fritz, P., Frape, S.K., 1982. Saline groundwaters in the Canadian Shield – a first overview. Chem. Geol. 36, 179–190.

Fuge, R., 1978. Bromine, in: Wedepohl, K.H. (Ed), Handbook of Geochemistry II/3, B-K

Gast, R.E., 1988. Rifting; im Rotliegenden Niedersachsens. Geowiss. 6, 103–136.

Gast, R.E., 1991. The perennial Rotliegend salt lake in NW Germany. Geol. Jb. A. 25–59.

Gat, J.R., 1975. Elucidating salinization mechanisms by stable isotope tracing of water sources. Int. Symp. Brakish Water as a Factor in Development, Beer Sheva 5.–10. Jan., pp. 15–23.

Gaupp, R., Gast, R., Forster, C., 2000. Late Permian playa lake deposits of the southern Permian Basin (Central Europe). Lake basins through space and time, in: Gierlowski-Kordesch, E.H., Kelt, K.R. (Eds), AAPG Studies in Geol. 46, pp. 5–86.

Gaupp, R., Matter, A., Platt, J., Ramseyer, K., Walzbuck, J.P., 1993. Diagenesis and fluid evolution in deeply buried Permian (Rotliegende) gas reservoirs, Northwest Germany. Amer. Assoc. Geol. Bull. 77, 1111–1128.

Gebhardt, U., 1994. Origin of the Rotliegend halites in the North German Basin (Upper Rotliegend II, Permian). Freiberg Forsch. H., C, 452, 3–22.

Geißler, M., Breitkreutz, C., Kiersniwski, H., 2008. Late Paleozoic volcanism, in the central part of the southern Permian Basin (NE Germany, W Poland): facies distribution and volcano-topographic hiati. Int. J. Earth Sci. 97, 973–989.

Giggenbach, W.F., 1992. Isotope shifts in waters from geothermal and volcanic systems along convergent plate boundaries and their origin. Earth Planet. Sci. Lett. 113, 495–510.

Glennie, K.W., Buller, A.T., 1983. The Permian Weissliegend of N.W. Europe: the partial deformation of aeolian dune sands caused by the Zechstein transgression. Sediment. Geol. 35, 43–81.

Graham, C.M., Sheppard, S.M.F., 1980. Experimental hydrogen isotope studies II: fractionations in the systems epidote-NaCl-H_2O, epidote-$CaCl_2$-H_2O and epidote-seawater, and the hydrogen isotope compositions of natural epidotes. Earth Planet. Sci. Lett. 49, 237–251.

Handford, C.R., 1982. Sedimentology and evaporate genesis in a Holocene continental-sabkha playa basin –Bristol Dry Lake, California. Sediment. 29, 239–253.

Hardie, L.A., Eugster, H.P., 1970. The evolution of closed basin brines. Mineral. Soc. Am. Spec. Pub. 3, 273–290.

Helgeson, H.C., Delany, J.M., Nesbitt, H.W., Nird, D.K., 1978. Summary and critique of the thermodynamic properties of rock-forming minerals. Amer. J. Sci. 278-A, USA.

Holser, W., 1979. Trace elements and isotopes in evaporates, in: Burns, R.G. (Ed.), Marine Minerals Reviews in Mineralogy. Mineral. Soc. Amer., 295–346.

Iannace, A., Gasparrini, M., Gabellone, T., Mazzoli, S., 2012. Late dolomitization in basinal limestones of the southern Appennines fold and trust belt (Italy). Oil & Gas Sci. Tech.-Rev IFP Energies nouvelles 67, 59–75.

Jacobson, G., 1988. Hydrology of Lake Amadeus, a groundwater discharge play in central Australia. J. Aust. Geol. Geophys. 10, 301–308.

Jones, B.F., Deocampo, M.D., 2003. Geochemistry of saline lakes, in: Holland, H.D., Turekian K.K. (Eds), Treatise on Geochemistry 5, 393-424.

Jones, B.F., Naftz, D.L., Spencer, R.J., Oviatt, C.G., 2009. Geochemical evolution of the Great Salt Lake, Utah, USA. Aquat. Geochem. 15, 95-121.

Kaufmann, R., Frape, S.K., Fritz, P., Bentley, H., 1987. Chlorine stable isotope composition of Canadian Shield brines, in: Fritz, P., Frape S.K. (Eds), Saline water and gases in crystalline rocks. GCA Spec. Pap. 33, 89–94.

Kelly, D.S., Karson, J.A., Blackman, D.K., Fruh-Green, G.I., Butterfield, D.A., Hayes, J.M., Lilley, M.D., Olson, E.J., Schrenk, M.O., Roe, K.K., Lebon, G.T., Rizzigno, P. 2001. An off-axis hydrothermal vent field near the Mid-Atlantic Ridge at 30°N. Nature 412, 154–149.

Kharaka, Y.K., Hanor, H.S., 2003. Deep fluid in the continents: I. Sedimentary basins, in: Holland, H.D., Turekian K.K. (Eds), Treatise on Geochemistry 5, 499-540.

Kharaka, Y.K., Maest, A.S., Carother, W.W., Law, L.M., Lamothe, P.J., Fries, T.L., 1987. Geochemistry of metal-rich brines from central Mississippi Salt Dome basin, USA. Appl. Geochem. 2, 543–561.

Kloppmann, W., Girard, J.-P., Negrel, P., 2002. Exotic stable istope compositions of saline waters and brines from the crystalline. Chem. Geol. 184, 49–70.

Kloppmann, W., Negrel, P., Casanova, J., Klinge, H., Schelkes, K., Guerrot, C., 2001. Halite dissolution derived brines in the vicinity of a Permian salt dome (N German Basin) Evidence from boron, strontium, oxygen and hydrogen isotopes. Geochim. Cosmochim. Acta 65, 4087–4101.

Le Maitre, R.W., Streckeisen, A., Zanettin, B., Le Bas, M. J., Bonin, B., Bateman, P., Bellieni, G., Dudek, A., Efremova, S., Keller, J., Lamere, J., Sabine, P. A., Schmid, R., Sorensen, H., Woolley, A.R., 2002. Igneous Rocks: A Classification and Glossary of Terms, Recommendations of the International Union of Geological Sciences, Subcommission of the Systematics of Igneous Rocks. Cambridge University Press, United Kingdom, 2nd Edt, 256 pp.

Li, J., Lowenstein, TK, Blackburn, J.R., 1997. Responses of evaporate mineralogy to inflow water sources and climate during the past 100 ky in Death Valley California. Geol. Soc. Am. Bull. 109, 1361–1371.

Lowenstein, T.K., Risacher, F. 2009. Closed basin brine evolution and the influence of Ca-Cl inflow waters: Death Valley and Bristol Dry Lake California, Qaidam Basin, China, and Salar de Atacama, Chile. Aquat. Geochem. 15, 71–94.

Lüders, V., Plesson, B., Romer, R.L., Weise, S.M., Banks, D.A., Hoth, P., Dulski, P., Schettler, G., 2010. Chemistry and isotopic composition of Rotliegend and Upper Carboniferous formation waters from North German Basin. Chem. Geol. 276, 198–208.

Lyons, W.B, Mayewski, P.A, 1993. The geochemical evolution of terrestrial waters in the Antarctic: the role of rock-water interaction. Physical and biogeochemical processes in antartic Lakes. Antarct. Res. Ser. 59, 135–143.

Matsubaya, O., Sakai, H., Toril, T., Burton, H., Kerry, K., 1979. Antarctic saline lakes - stable isotopic ratios, chemical composition and evolution. Geochim. Cosmochim. Acta 43, 7–25.

McCaffrey, M.A., Lazar, B., Holland, H.D., 1987. The evaporation path of seawater and the coprecipitation of Br^- and K^+ with halite. J. Sediment. Petrol. 57, 928–937.

McCann, T., 1998. Sandstone composition and provenance of the Rotliegend of the NE German Basin. Sediment. Geol. 116, 177–198.

Möller, P., Rosenthal, E., Geyer, S., Flexer, A. (2007) Chemical evolution of saline water in the Jordan-Dead Sea transform and in adjoining areas. Int. J. Earth Sci. 96, 541-566; 593-597.

Möller, P., Weise, S.M., Althaus, E., Bach, W, et al., 1997. Paleofluids and recent fluids in the upper continental crust: results from the German Continental Deep Drilling Program. J. Geophys. Res. 102, B8, 18233–18254.

Möller, P., Weise, S.M., Tesmer, M., Dulski, P., Pekdeger, A., Bayer, U., Magri, F., 2008. Salinization of groundwater in the North German Basin: results from conjoint investigations of major, trace elements and multi-isotope distribution. Int. J., Earth Sci. 97, 1057–1073.

Möller, P., Woith, H., Dulski, P., Lüders, V., Erzinger, J., Kämpf, H., Pekdeger, A., Hansen, B., Lodemann, M., Banks, D., 2005. Main and trace elements in KTB-VB fluid: Composition and hints to its origin. Geofluids 5, 28–41.

Oberhänsli, H., Weise, S. M., Stanichny, S., 2009. Oxygen and hydrogen isotopic water characteristics of the Aral Sea, Central Asia. J. Mar. Syst. 76, 310–321.

Paces, T., 1987. Hydrochemical evolution of saline waters from crystalline rocks of the Bohemian Massif (Czechoslovakia), in: Fritz, P., Frape, S.K. (Eds), Saline water and gases in crystalline rocks. Geol. Ass. Canada Spec. Pap. 33, 145–156.

Parkhurst, D.L., Appelo, C.A.J., 2010. User's Guide to PHREEQC (Version 2.17.5)-A Computer program for speciation, batch-reaction, one-dimensional transport and inverse geochemical calculations. http://www.brr.cr.usgs.gov/projects/GWC_coupled/phreeqc/index.html

Pierret, M.C., Clauer, N., Bosch, D., Blanc, G., France-Lanord, C., 2001. Chemical and isotopic ($^{87}Sr/^{86}Sr$, $\delta^{18}O$, δD) constraints to the formation processes of Red-Sea Brines. Geoch. Cosmoch. Acta 65, 1259.

Plein, E., 1978. Rotliegend Ablagerungen im Norddeutschen Becken. Z. dt. geol. Ges., 129, 71–97.

Rank, D., Özsoy, E., Saligoğlu, I., 1999. Oxygen-18, deuterium and tritium in the Black Sea and the Sea of Marmara. J. Environ. Radioactiv. 43, 231–245.

Regenspurg, S., Feldbusch, E., Norden, B., Tichomirowa, M., 2016. Fluid-rock interactions in a geothermal Rotliegend/Permo-Carboniferous reservoir (Geman Basin). Appl. Geochem. 69, 12–27.

Richet P., Bottinga Y Javoy M., 1977. A review of H, C, N, O, S, and Cl stable isotope fractionation amoung gaseous molecules. Ann. Rev. Earth Planet. Sci. 5, 65–110.

Risacher, F., Alonso, H., Salazar, C. 2003. The origin of brines and salts in Chilean salars: by hydrochemical review. Earth Sci. Rev. 63, 249–293.

Risacher, F., Alonso, H., Salazar, C., 1999 Geoquimica de aguas en cuencas cerradas: I, II y III Regiones–Chile, S.I.T. Nr. 51, Santiago, 631 pp.

Salameh, E., Alraggad, M., Tarawneh, A., 2014. Natural salinity sources in the groundwaters of Jordan-importance of sustainable aquifer management. Chemie der Erde-Geochem. 74, 735–747.

Schmidt, G.A., 1999. Forward modeling of carbonate proxy data from planktonic foraminifera using oxygen isotope tracers in a global ocean model. Paleoceanography 14, 482–497.

Schmidt, K., Koschinsky, A., Garbe-Schönberg, D., de Carvalho, L.M., Seifert, R., 2007. Geochemistry of hydrothermal fluids from the ultramafic-hosted Logatchev hydrothermal field, 15°N on the Mid-Atlantic Ridge: Temporal and spatial investigation. Chem. Geol. 242, 1–21.

Shock, E.L., Helgeson, H.C., 1988. Calculation of the thermodynamic and transport properties of aqueous species at high pressures and temperatures: Correlation algorithms for ionic species and equation of state predictions to 5 kb and 1000°C. Geochim. Cosmochim. Acta 52, 2009–2036.

Sieland, R., 2014. Hydraulic investigations of the salar de uyuni, Bolivia. Freiberg Online Geosci. 37.

Simon, K., Hoefs, J., 1993. O, H, C isotope study of rocks from KTB pilot hole: crustal profile and constraints on fluid evolution. Contrib. Mineral. Petrol. 114, 42–52.

Sofer, Z., Gat, J.R., 1972. Activities and concentrations of oxygen-18 in concentrated aqueous salt solutions: analytical and geophysical implications. Earth Planet. Sci. Lett. 15, 232–238.

Sofer, Z., Gat, J.R., 1975. The isotope composition of evaporating brines: effect of the isotope activity ratio in saline solutions. Earth Planet. Sci. Lett. 26, 179–186.

Spencer, R.J., Lowenstein, T.K., Casas, E., Zhang, P., 1990. Origin of Potash salts and brines in the Qaidam Basin, China, in: Spencer, R.J., Chou, I. (Eds), Fluid mineral interaction: A tribute to H.P. Eugster, Geochem. Soc. (London) Spec. Publ. 2, 395–408.

Stotler, R.L., Frape, S.K., Ruskeeniemi, T., Ahonen, L., Onstott, T.C., Hobbs, M.Y., 2009. Hydrogeochemistry of groundwaters in and below the base of thick permafrost at Lupin, Nunavut, Canada. J. Hydrol. 373, 80–95.

Tivey, M.K, 2007. Generation of seafloor hydrothermal vent fluids and associated mineral deposits. Oceanography 20, 50–65.

Toner, D.T., Sletten, R.S., 2013. The formation of Ca-Cl rich groundwater in the Dry Valleys of Antarctica: Field measurements and modelling of relative transport. Geochim. Cosmochim. Acta 110, 84–105.

Van Wees, J.-D, Stephenson, R.A., Ziegler, P.A., Bayer, U., McCann, T., Dadlez, R., Gaupp, R., Narkiewicz, M., Bitzer, F., Schreck, M., 2000. On the origin of the Southern German Permian Basin, Central Europe. Mar. Petrol. Geol. 17, 43–59.

Warren, J.K., 2008. Salt as sediment in the central European Basin system as seen from a deep time perspective, in: Littke, R., Bayer, U., Gajewski, D., Nelskamp, S. (Eds) Dynamics of complex interacontinental basins. Springer, Berlin Heidelberg, pp. 249–276.

Webster, J.G., 1994. Trace element behaviour in oxic and anoxic Ca-Cl brines of the Wright Valley drainage, Antarctica. Chem. Geol. 112, 255–274.

Wimmenauer, W., 1985. Petrographie der magmatischen und metamorphen Gesteine. Enke Verlag.

Ziegler PA (1990): Geological Atlas of Western and Central Europe - second revised edition. The Hague.

Ziegler, P.A., 1977. Geology and hydrocarbon provinces of the North Sea. GeoJ. 1, 7-32.